Thermochimica Acta, 220 (1993) 117–130
Elsevier Science Publishers B.V., Amsterdam

Kinetic parameterization of transitions and reactions in food systems from isothermal and non-isothermal DSC traces

Marco Riva and Alberto Schiraldi *
DISTAM–University of Milan, Via Celoria 2, 20133 Milan (Italy)

(Received 1 October 1992; accepted 16 October 1992)

Abstract

When reactions and/or transitions take place within a food system, i.e. in the presence of a number of components, their kinetic parameterization can be approached by careful analysis of isothermal DSC traces. Even when the signal is relatively smooth, a "fine structure" can be observed. This can be used in numerical manipulations if the original trace is in digital format. Some simple expressions are proposed for the determination of kinetic parameters from isothermal and non-isothermal scans. The case of consecutive reactions is also considered.

INTRODUCTION

The kinetic parameterization of a process, together with an estimation of its enthalpy, has often been determined from DSC traces obtained at a given heating rate, i.e. under non-isothermal conditions.

The determination is generally based on the assumption that the process that takes place in the course of the DSC scan may be treated as a reversible transition. This is the case, for instance, for protein unfolding in aqueous solution which has been analysed via the van't Hoff equation by a number of authors [1–3]. This approach underlies the analysis of the experimental traces, including their deconvolution into a number of more simple functions, to yield the relevant kinetic order and activation energy. Despite the unsatisfactory application of thermodynamic and kinetic relationships within the same context and, possibly as a result of internal compensations, e.g. due to the unavoidable correlation among different parameters, this procedure may give a self-consistent description of the process investigated.

A peculiarity of these approaches is the focus of attention on the calorimetric signal in the region of the peak maxima or minima, i.e. where the trace derivative is zero or constant. This leads to a number of

* Corresponding author.

simplifying assumptions, resulting in a satisfactory fit or justifying the observed trace trend.

More recently, an improved approach has been proposed by Sandu and Singh [4] who determined the kinetic parameterization by emphasising, as should always be the case, the direct connection between calorimetric signal and the reaction rate. The mathematical procedure proposed by these authors is however difficult to use when the DSC signal reveals a multi-stage process, i.e. when several thermal effects are present in the overall trace observed.

As a final comment, it must be emphasised that there are few literature reports of kinetic parameterization of isothermal DSC traces [5–7].

The present work reports some suggestions for kinetic parameterization of isothermal and non-isothermal DSC traces without the use of any "theoretical" model. Therefore, the suggestions should be applicable to complex cases such as those in biological and food systems, where reactions and transitions take place in the presence of a number of components.

The examples reported here concern protein denaturation within natural systems, such as the white of hen eggs and beef muscle, investigated at a constant heating rate, and starch gelatinization, monitored in either isothermal or non-isothermal conditions. The sample preparation and experimental details are reported elsewhere [7–9].

METHODS

A Mettler DSC 20 and a Setaram C80 D were employed for the non-isothermal and isothermal investigations, respecively. In both cases, the calorimetric trace was converted into digital format for numerical manipulation in a worksheet software. For this work, the DSC trace was formatted as an ASCII file and analysed using a LOTUS 123 worksheet.

Owing to the complexity of the systems considered, the trace baseline across the signal was approximated either with a straight line, when a small drop (compared with the peak height) was observed between pre- and post-signal trends, or with an SP-line for larger drops, and subtracted from the experimental trace. The scaled trace, still in the form of worksheet data vectors (temperature/time and signal), was submitted to a non-linear regression analysis through a STATGRAPHICS routine for its deconvolution into a number of gaussian functions. Although these cannot exactly reproduce the onset and the end of a DSC peak, the error implied does not significantly affect the evaluation of the enthalpy [10] and the kinetic parameters.

The number of gaussian functions required to fit a given trace should be the number of transformations expected to occur in the temperature range considered. For the actual cases treated in this paper, the relevant literature suggests that many of the proteins undergo denaturation simultaneously, e.g. ovomucoids with conalbumin, sarcoplasmic proteins with collagen, etc.,

so that the respective thermal effects completely overlap one another and cannot be separated. The size of the function set was therefore kept as small as possible to attain a reasonable fitting accuracy. Accordingly, each gaussian contribution did actually correspond to denaturation of a group of proteins present in the sample.

Further manipulation to yield kinetic parameters from the deconvoluted traces was carried out by means of a MATCAD routine.

DISCUSSION

A simple one-step chemical or physical process

$$A \rightarrow B$$

is accompanied by an enthalpy change proportional to the mass of B, such that

$$Q = m(B)\,\Delta_r H$$

where $\Delta_r H$ is the enthalpy change relative to the unit mass, which is assumed to be independent of the temperature T in the case of non-isothermal DSC scans. If $m_t(B)$ is the total mass of B produced on completion of the process, the total heat released or adsorbed by the system will be

$$Q_\infty = m_t(B)\,\Delta_r H$$

If the extent of reaction is

$$\alpha = \frac{m(B)}{m_t}$$

then

$$\alpha = \frac{Q}{Q_\infty}$$

The calorimetric signal above the chosen baseline is

$$s = \frac{dQ}{dt} = Q_\infty \frac{d\alpha}{dt}$$

where t is the time.

Accordingly

$$Q = \int_{t_o}^{t} s\,dt \quad \text{and} \quad Q_\infty = \int_{t_o}^{t_e} s\,dt$$

where t_o and t_e are the onset and the end point of the signal. The rate of process is therefore

$$V = \frac{d\alpha}{dt} = K(1-\alpha)^n = \frac{s}{Q_\infty} \qquad (1)$$

where K and n are the kinetic constant and the kinetic order, respectively. This equation holds either for isothermal or non-isothermal scans.

Due to the delay in heat transfer from the sample to the thermocouples set beneath (Mettler DSC) or around (SETARAM C80) the calorimetric cells, the temperature of a DSC record should be corrected, especially at the starting point of the scan, to reproduce the actual temperature of the sample. When the instrument used has a small thermal lag, as in the case of the Mettler DSC 20, the actual temperature scan rapidly attains the pre-fixed program with a constant, small gap that does not affect the shape of the DSC trace. The temperature difference between sample and thermocouple may nonetheless change with temperature and should be accounted for in defining the baseline [4].

Accordingly, once amended the trace reproduces the thermal history of the sample. The starting point of a transition is revealed by a downward or upward shift from the baseline. This is significant when a threshold value (according to the sensitivity of the instrument used), s_{tr}, is reached which corresponds to a threshold rate, V_{tr}.

When a system undergoes a temperature scan, it moves from the condition where $\Delta_r G > 0$ (the process is thermodynamically impossible because of the positive difference of the Gibbs function G) to that where $\Delta_r G < 0$, namely, below and beyond the onset temperature T_o, respectively. The appearance of a DSC signal occurs when $\Delta_r G \leq 0$ and $V \geq V_{tr}$.

When the scan goes through the temperature T_{eq} at which $\Delta_r G = 0$, the system is subjected to the smallest driving force and the rate of reaction is accordingly the lowest. This implies $T_{eq} \leq T_o$. Were the system kept at T_o, the activities of the reagents and products would slowly attain their own equilibrium values. But, because the scan has a finite rate, the system will go through T_o driven by a force that increases with T. The rate of reaction will therefore rise to a maximum (which corresponds to the peak maximum or minimum) at T_m, mainly because of temperature increase, slowing down after T_m and finally vanishing at T_e, because of the progressive exhaustion of unreacted mass.

Non-isothermal scans

Equation (1) may be rewritten in differential form

$$\frac{d \ln V}{d(1/T)} = \frac{d \ln K}{d(1/T)} + n \frac{d \ln(1-\alpha)}{d(1/T)}$$

$$= -\frac{\Delta E_a}{R} + n \frac{d \ln(1-\alpha)}{d(1/T)} = \frac{d \ln s}{d(1/T)} \qquad (2)$$

where the Arrhenius law has been assumed for K. Because the T and s values are stored as data vectors in a worksheet, it is very simple to generate associate vectors for Q_∞, $\ln s$, $(1/T)$, $(1-\alpha)$ and $\ln(1-\alpha)$, and, in addition, for the relevant derivatives, either versus T or $(1/T)$. These derive directly from the experimental data and are known quantities. Thus,

$d \ln(1-\alpha)/d(1/T)$ (Y_T) and $d \ln s/d(1/T)$ (X_T) can be fitted according to a straight line

$$Y_T = \frac{1}{n} X_T + \frac{\Delta E_a/R}{n} \tag{3}$$

whose slope and intercept are equal to $1/n$ and $\Delta E_a/nR$, respectively.

A peculiar feature of this approach is that it does not require any underlying model except for the Arrhenius law. It should, however, be applied only when the process considered is simple, i.e. there are no intermediate steps or independent processes taking place in the same temperature range — a very rare situation when dealing either with large biopolymers that undergo conformational and phase transitions, or with natural mixtures of biopolymers that can mutually interact and are affected by other solutes.

Figure 1 reports the case for potato starch gelatinization, which, for a 5 K min^{-1} heating rate, gives $n = 1.28$ and $\Delta E_a = 315.2$ kJ mol^{-1}. It must be

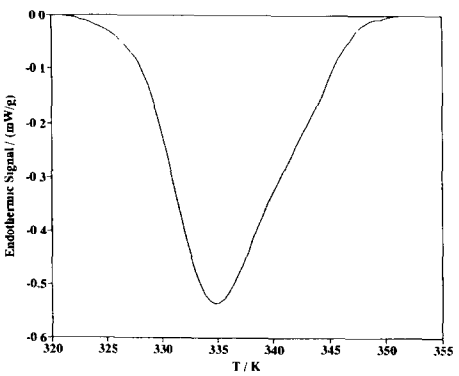

(a)

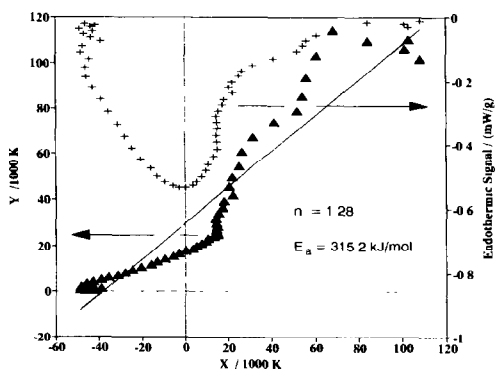

(b)

Fig. 1. a. DSC traces of starch–water (30% w/w) sample recorded at 5°K min^{-1} heating rate. b. Endothermic signal and corresponding scaled signal in the plane (X,Y). Crosses and triangles are the digital experimenal data of DSC scan recorded at 5°K min^{-1}.

stressed that these quantities have a phenomenological meaning and do not allow any detailed consideration of the mechanism of the process. In spite of the simple shape of the calorimetric signal, the case of starch-gelatinization is indeed rather intriguing, because it is a multi-stage process in which the glass transition of the starch is followed by amylopectin "fusion" and, at higher temperatures, by crystallization of amorphous amylose [11]. When the starch/water ratio is smaller than 30% (w/w), the DSC trace shows a rather regular single peak, which has been used to approach the kinetic parameterization of the overall process [12].

Careful inspection of the trace, however, reveals some minor "irregularities" in the peak profile (Fig. 1a). When the signal is replotted against X_T peak profile is modified (Fig. 1b, upper part), but not as expected for a pure gaussian profile (see examples given below). In other words, the data treatment allows us to recognize the underlying complexity of an apparently simple signal.

When a glass transition can be excluded, the calorimetric traces of biological tissues and/or solutions require deconvolution in more contributions that, for practical purposes (see Methods section), may be assumed to have a gaussian trend

$$s_i = s_{m,i} \exp\left(-\frac{(\delta T)_i^2}{2\sigma_i^2}\right)$$

with $(\delta T)_i = (T - T_{m,i})$, where $s_{m,i}$, $T_{m,i}$ and σ_i are height, mean temperature and standard deviation of the ith gaussian function of the set used for the deconvolution.

Figures 2 and 3 report the case of protein denaturation in the white of

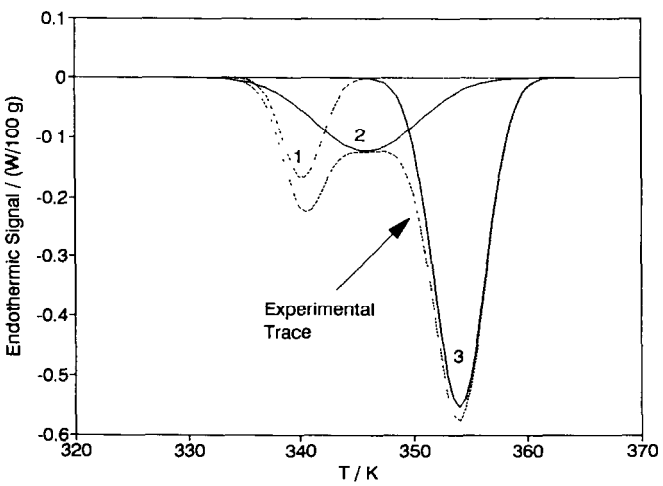

Fig. 2. Protein denaturation of hen egg white. DSC trace deconvoluted into three gaussian components.

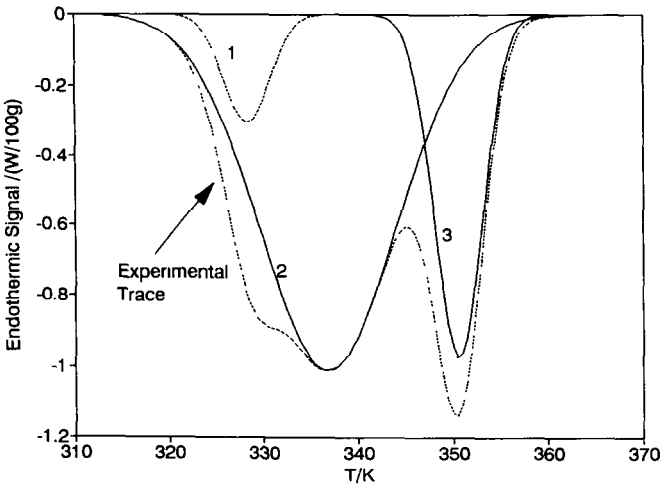

Fig. 3. Protein denaturation in beef muscle. DSC trace deconvoluted into three gaussian components.

hen eggs and in beef muscle, respectively. In each case, the literature suggests deconvolution in three main contributions [10, 13] although the actual number of proteins undergoing denaturation is, especially for beef muscle, higher.

Once the sum of the gaussians that fits the trace is assessed, the above procedure for the kinetic parameterization is largely simplified, as one no longer needs worksheet manipulation of the experimental data to obtain α, $\ln(1-\alpha)$ and its derivative versus $1/T$ for each single gaussian contribution.

It is easy to recognize that, in this case

$$X_T = \frac{T^2(\delta T)_i}{\sigma_i^2}$$

$$Y_T = \frac{s_i T^2}{s_{m,i}\sigma_i\sqrt{2\pi}} \qquad \frac{1}{(1-\alpha_i)}$$

which via eqn. (3) gives

$$\Delta E_{a_i} = \frac{2n_i R T_{m,i}^2}{\sigma_i\sqrt{2\pi}} \tag{4}$$

which accounts for the predicted correlation [4] between peak skewness (σ_i in this approach), kinetic order and activation energy.

Taking into account the peculiar value of the defined integral of the gaussian function across the range $[(T_{m,i}+\sigma_i), (T_{m,i}-\sigma_i)]$, the equalities:

$$X_T(T_{m,i}+\sigma_i) = \frac{(T_{m,i}+\sigma_i)^2}{\sigma_i}$$

and

$$Y_T(T_{m,i} + \sigma_i) = \frac{(T_{m,i} + \sigma_i)^2 \exp(-0.5)}{0.158\sigma_i\sqrt{2\pi}}$$

can be deduced, which permit the evaluations of n_i and ΔE_{a_i}.

Equation (3), accordingly rewritten as

$$Y_T = \frac{2T_{m,i}^2}{\sigma_i\sqrt{2\pi}} + \frac{T^2(\delta T)_i}{n_i\sigma_i^2} \tag{5}$$

allows representation and direct comparison of various gaussian contributions to the DSC trace in the same Y_T vs. X_T plane. The corresponding plots are straight lines that allow the evaluations of n and ΔE_a from the slope and intercept on the Y_T axis, respectively.

Figures 4 and 5 show the Y_T vs. X_T plots for the egg white and beef muscle, respectively, and Table 1 summarizes the relevant kinetic parameters.

Isothermal scans

For a simple isothermal process, eqn. (1) indicates that the calorimetric signal has its largest value s_m at $t = 0$, for any kinetic order

$$s(t = 0) = KQ_\infty = s_m \tag{6}$$

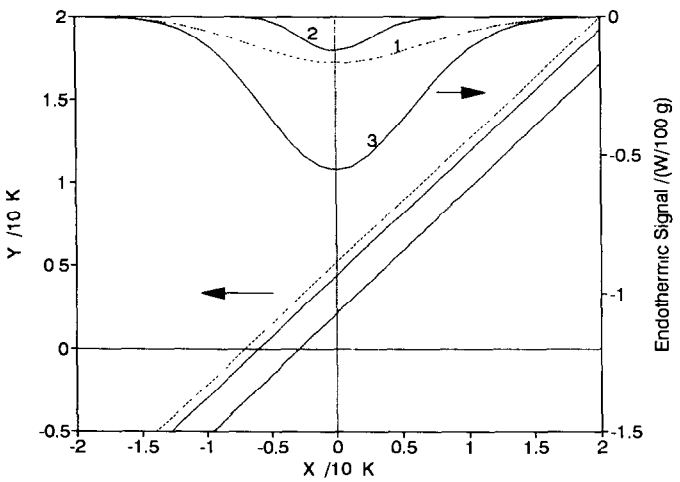

Fig. 4. Hen egg white DSC gaussian components scaled in the plane (X,Y). The straight lines correspond to eqn. (5).

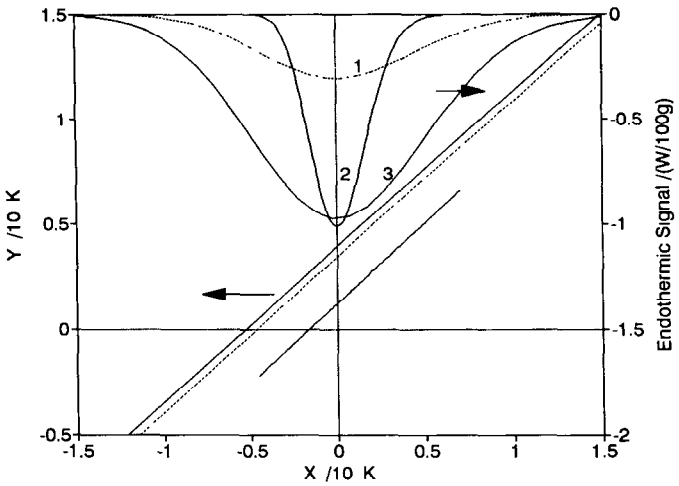

Fig. 5. Beef muscle DSC gaussian components scaled in the plane (X,Y). The straight lines correspond to eqn. (5).

and

$$V = \frac{d\alpha}{dt} = \frac{Ks}{s_m} \tag{7}$$

Accordingly, the "ideal" calorimetric signal should be

$$F_0(t) = s_m$$

$$F_1(t) = s_m \exp(-Kt)$$

$$F_2(t) = s_m\left(1 - \frac{Kt}{1+Kt}\right)^2$$

for $n = 0$, $n = 1$ and $n = 2$, respectively.

However, the trend of the actual signal is somewhat delayed with respect

TABLE 1

Kinetic parameters for the protein denaturation of egg white and beef muscle obtained from the Y_T vs. X_T plots in Figs. 4 and 5, respectively

	n	ΔE_a (kJ mol^{-1})
Egg white		
Conalbumin	1.36	594.5
Lysozime	1.33	244.6
Ovoalbumin	1.35	504.6
Beef muscle		
Light myosin	1.35	389.2
Sarcoplasmic and collagen	1.31	137.8
Actomyosin aggregates	1.35	442.4

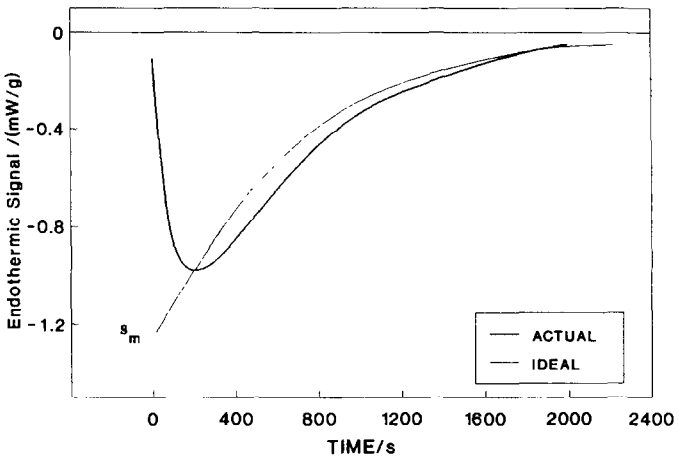

Fig. 6. Actual and ideal DSC signals for an isothermal reaction. The actual signal accounts for the lag time of the calorimeter used.

to "ideality" because of the time constant of the instrument used. This may easily be accounted for if the above expressions are multiplied by a dumping function, such as $\exp(-\tau/t)$, where τ is the time constant of the instrument. Figure 6 represents a simulation of actual signals.

Taking into account eqns. (6) an (7), integration of eqn. (1) gives

$$\alpha = 1 - \frac{s}{s_m}[(n-1)Kt + 1]$$

If this expression is differentiated and compared with eqn. (7), a straightforward manipulation yields

$$\frac{s}{D} = \frac{1-n}{n}t - \frac{1}{Kt} \tag{8}$$

where $D = \mathrm{d}s/\mathrm{d}t$.

Equation (8) is rather useful because it holds for any kinetic order and allows the ratio s/D (easily assembled through a worksheet manipulation of the experimental trace data) to be plotted against t, yielding a straight line from which both n and K can therefore be evaluated.

Figure 7 represents a simulation of processes with the same s_m and K, but with different n values.

The real case of starch gelatinization is reported in Fig. 8; the trace refers to starch gelatinization at 95°C, i.e. well above the temperature of the starch glass transition and amylose crystallization. The process therefore only concerns the water-assisted fusion of starch crystallites. The fit of the experimental data reported in Fig. 8 corresponds to first-order kinetics. The large scatter of data just above $t = 0$ is due to the thermal lag of the calorimetric response not accounted for in eqn. (8). The actual situations

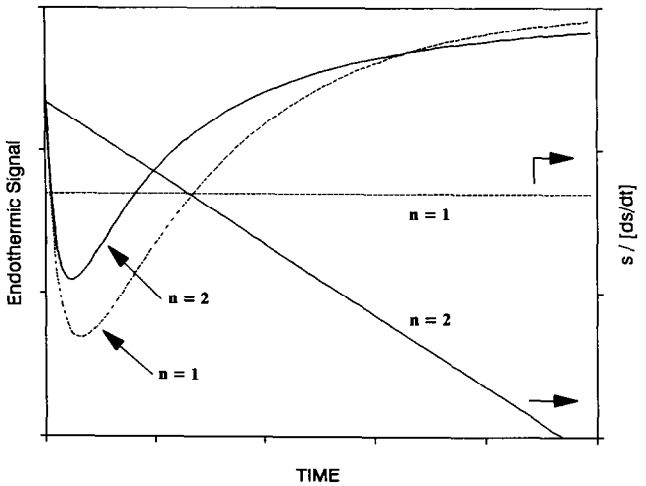

Fig. 7. Simulation of endothermic signals corresponding to reactions with different kinetic orders (n) and equal enthalpies of reaction and kinetic constants.

thus require use of eqn. (8) to achieve a tentative evaluation of n and K ($n = 1$ and $K = 0.00154\,s^{-1}$ for the data in Fig. 8). The trace data should then be treated according to the appropriate equation

$$s = \exp(-\tau/t)F_n(t)$$

This procedure gives the τ, s_m, n and K values that allow the best fit of the whole trace. Q_∞ is accordingly evaluated as s_m/K. Figure 9 shows a comparison of the experimental and calculated traces for isothermal starch gelatinization: $n = 1$ is therefore confirmed, while $K = 1.93 \times 10^{-3}\,s^{-1}$ is

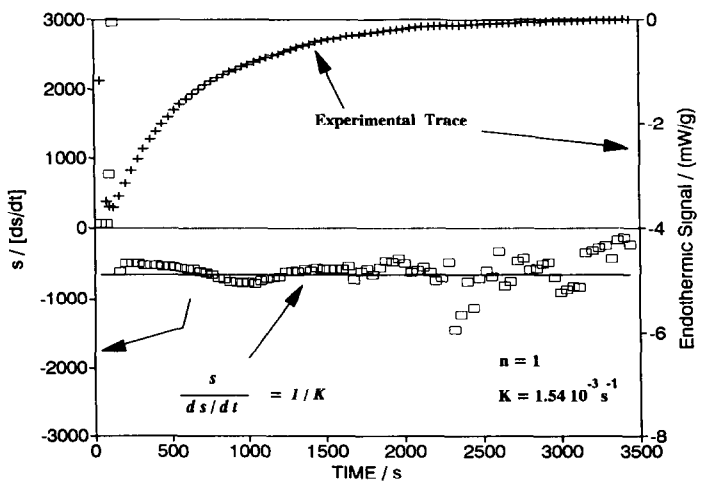

Fig. 8. Upper: DSC trace of isothermal starch gelatinization. Lower: DSC scaled signal according to eqn. (8).

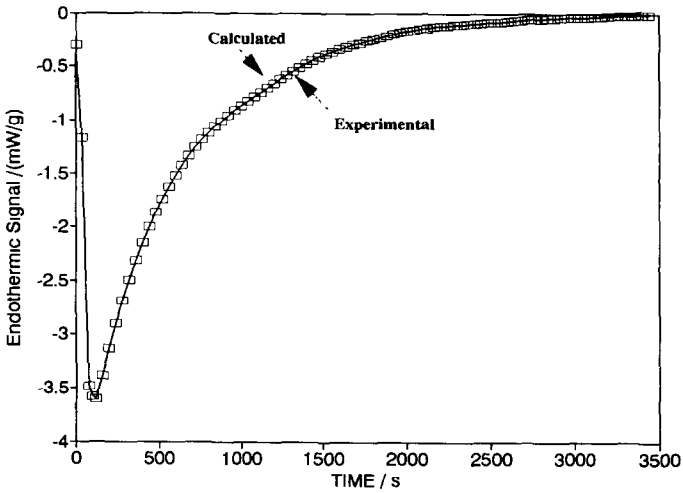

Fig. 9. Experimental and calculated DSC trace for isothermal starch gelatinization.

larger than the above tentative value. The lag time of the calorimetric response is $\tau = 39.2$ s; the maximum ideal signal is $s_m = -5.61$ mW g^{-1}, and the overall thermal effect is $Q_\infty = 2.9$ J g^{-1} (referred to pure starch).

Equation (1) permits other considerations. When rewritten in the form

$$s = F_n(t) = s_m(1 - \alpha)^n$$

it predicts the s value (of the "ideal" trace) at the half-life time $t_{1/2}$, namely, $0.5s_m$ and $0.25s_m$ for $n = 1$ and $n = 2$, respectively. Figure 10 reports simulated cases.

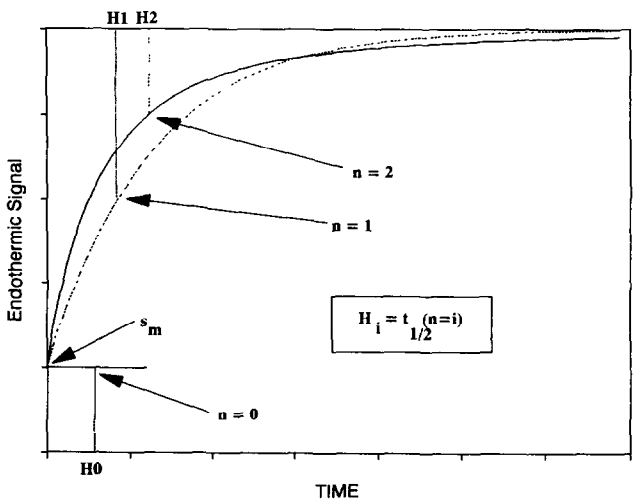

Fig. 10. Ideal DSC traces corresponding to reactions of different kinetic order; H_0, H_1 and H_2 are the respective half-lives.

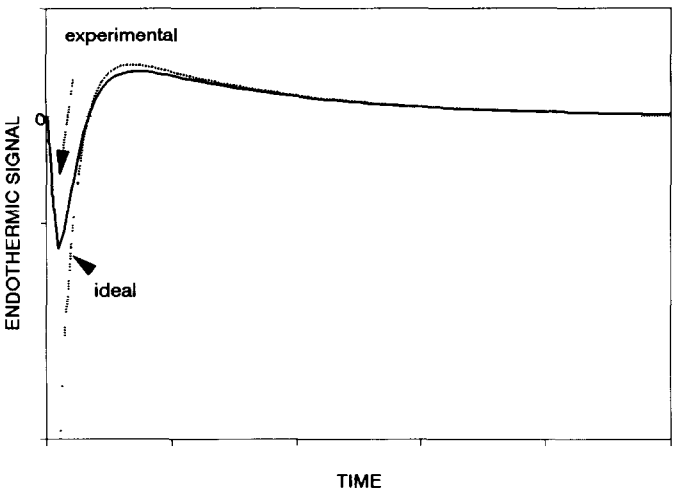

Fig. 11. Isothermal DSC trace for two first-order consecutive reactions with thermal effects of opposite sign.

DSC traces become rather more complex when more processes take place in the same system: this is the case for consecutive reactions, either in the classic sense, or in that of reactions induced only after exhaustion of a previous stage, such as yeast growth. The former has been fully discussed by Sandu and Singh [4] for non-isothermal conditions. Here we simply apply the above treatment to each stage of a consecutive reaction path; i.e. direct use of the classical expression for the reaction rate, which is then multiplied by the corresponding reaction enthalpy to generate an expression for the "ideal" DSC signal $F(t)$. This is finally multiplied by the dumping function $\exp(-\tau/t)$ to attain the trend of the actual DSC trace.

Figure 11 reports the example of two first-order consecutive reactions with thermal effects of opposite sign (−2.7 J and 0.3 J, respectively), deliberately chosen to show that, in such extreme conditions, the actual treace presents an initial waving trend that might be misinterpreted as a starting noise of the recording. The kinetic constants (1.5×10^{2} and $1.5 \times 10^{-2}\,s^{-1}$) and reaction enthalpies have been chosen to simulate a situation where actual and ideal DSC traces are significantly different from each other in the early part of the process, while becoming very close later on. This means that the occurrence of a "small" signal with some waving noise at the start of the trace should be carefully considered.

CONCLUSIONS

It can be concluded that, once the expressions for reaction rates have been assessed, a regression analysis can be applied to fit the whole DSC trace. The adjustable parameters depend on the kind of scan, isothermal or non-isothermal. In the former case, the delay of the calorimetric response

has to be accounted for, because it significantly affects the initial part of the trace.

As for non-isothermal scans, a previous choice of the baseline is required. Although a straight line across the onset and end points of the whole signal may be a reasonable baseline, some uncertainty could come from glass transitions that sometimes take place just before the onset of peaks, as in the case of starch gelatinization.

The procedures proposed in this paper, however, allow recognition of such occurrences and therefore seem adequate to treat many kinds of DSC traces. Their use for the parameterization of traces from microbial growth is in progress.

ACKNOWLEDGEMENTS

This research was supported by the National Research Council of Italy, Special Project RAISA, Subproject 4, Paper No. 662.

REFERENCES

1 H.J. Borchardt and F. Daniels, J. Am. Chem. Soc., 79 (1957) 41.
2 P.L. Privalov, Adv. Prot. Chem., 33 (1979) 167.
3 E. Freire and R.L. Biltonen, Biopolymers, 17 (1978) 463, 481, 497
4 C. Sandu and R.K. Singh, Thermochim. Acta, 159 (1990) 267.
5 P.C. Gravelle, J. Therm. Anal., 14 (1978) 53–77.
6 J. Rouquerol, S. Partyka and F. Rouquerol, J. Chem. Soc., Faraday Trans. 1, 73 (1977) 306–313.
7 M. Riva, L. Piazza and A. Schiraldi, Cereal Chemistry, 68 (1991) 622.
8 A. Schiraldi and M. Rossi, Thermochim. Acta, 199 (1992) 115.
9 M. Riva, S. Terzi and A. Schiraldi, Ital. J. Food Sci., submitted for publication; see also, in M. Riva and A. Schiraldi (Eds.), Applicazioni della Calorimetria ai prodotti Alimentari, National Council of Research, Rome, Monografia RAISA 4/1, 1992, available free of charge upon request to the authors.
10 J.W. Donovan and K.D. Ross, J. Biol. Chem., 250 (1975) 6026.
11 L. Slade and H. Levine, CRC Crit. Rev. Food Sci. Nutr., 30 (1991) 115.
12 D.B. Lund, CRC Crit. Rev. Food Sci. Nutr., 20 (1984) 249.
13 C.J. Findlay and S. Barbut, in V.R. Harwalkar and C.-Y. Ma (Eds.), Thermal Analysis of Foods, Elsevier, London, 1990, p. 92.